Electronic Supplementary Information

Stacking of purines in water: the role of dipolar interaction in caffeine

L. Tavagnacco[ab], S. Di Fonzo[a*], F. D'Amico[a], C. Masciovecchio[a], J. W. Brady[c], A. Cesàro[ab]

[a]*Elettra-Sincrotrone Trieste S.C.p.A., Strada Statale 14 Km 163.5, Area Science Park, I-34149 Trieste, Italy*

[b]*Lab. of Physical and Macromolecular Chemistry, Department of Chemical and Pharmaceutical Sciences, University of Trieste, via L. Giorgieri 1, 34127 Trieste, Italy*

[c]*Department of Food Science, Stocking Hall, Cornell University, Ithaca, New York, 14853, USA*

[*]Corresponding author: Silvia di Fonzo

Elettra-Sincrotrone Trieste S.C.p.A., Strada Statale 14 Km 163.5, Area Science Park,

I-34149 Trieste, Italy

Tel +39-040-375-8816

e-mail: silvia.difonzo@elettra.eu

Table S1 Experimental wavenumbers from isotropic Raman data (at incident wavelength λ=266nm and λ=532 nm) for caffeine aqueous solutions at a concentration 1m and T=353 K. Simulation results: wavenumbers (cm^{-1}), IR Intensity, Raman Activity and their tentative vibrational assignments. Only wavenumbers for IR intensities and Raman activities >1 have been reported. In the assignment v stands for a stretching mode, ρ for a rocking mode and δ for a bending mode.

Raman experiment Isotropic profile Caffeine 1m, T=353 K		Results of simulations opt mp2/6-311++g(d,p), freq b3lyp/6-311++g(2d,2p)			Assignment
266. nm	532 nm	wavenumbers (cm^{-1})	IR Intensity	Raman Activity	
1 1031	1034	1036	80.2	3.9	ρ(C1M)+ v(N3-C3M)+v(C6-N1-C2)+δ(C8-H8)
2 1078	1079	1089	1.8	11.6	ρ(C1M,C3M, C7M) + δ(N-CH) + v (C8-N7)
3 1192	-	1209	18.9	1.7	δ(N-CH) + ρ(C3M) + v(N1-C1M) + v(N7-C7M)
4 1246	1241	1252	81.5	24	δ (CH-N) + ρ(C1M, C3M, C7M)
5 1258	1256	1265	17.2	15.3	v(C-N) + ρ(C1M, C3M, C7M)
6 1291	1291	1287	24.9	16.1	v(C–N) + v(C–C) in both rings + ρ(C3M)
7 1333	1332	1335	13.4	71.6	v(imidazole ring)
8 1363	1362	1372	94.1	18.5	v(C–N) + δ(C1M, C3M, C7M)
9 1393	1395	-	-	-	-
10 1409	1406	1405	18.1	2.4	v(imidazole ring) + v(CN) + δ(C1M, C3M, C7M) + δ(C8H8)
11 1437	1439	1440	106.5	23	δ(C1M, C3M, C7M) + δ(C8H8) + v(C–N)
		1456	21.3	5.4	
		1468	11.1	3.2	
		1484	98.7	3.6	
		1487	24.3	8.8	
12 1492	1497	1499	16.4	9.7	δ(C1M, C3M, C7M) + v(C–N)
		1501	12.34	7.96	
		1518	7.83	9.27	
		1519	5.98	12.00	
		1521	16.98	2.6	
13 1552	1549	1569	117.4	1.8	v(pyrimidine ring) + δ(C1M, C3M, C7M)
14 1601	1598	1590	97.2	50.3	v(C=C) + v(C–N) + δ(C1M, C3M, C7M)
15 1642	1647	1672	845	30.4	v(C=O) out of phase + v(C C)
16 1697	1692	1715	424.3	52.5	v(C=O) in phase

Table S2 Optimized geometrical parameters of caffeine obtained by Moller-Plesset (MP2) perturbation theory and 6-311++G(d,p) basis set. This optimization was used as input for calculation of the Raman normal modes.

```
---------------------------------------------------------------------
   Center      Atomic           Coordinates (Angstroms)
   Number      Number        X            Y            Z
---------------------------------------------------------------------
     1           7        -1.296082    -2.066270    -0.011430
     2           6        -0.348404    -1.092988    -0.050456
     3           6         1.853390    -0.172217    -0.008286
     4           8         3.066454    -0.284688     0.103729
     5           7         1.016742    -1.272296    -0.113852
     6           6         1.603844    -2.601014     0.046925
     7           1         1.869437    -2.783342     1.092384
     8           1         0.863627    -3.330533    -0.279891
     9           1         2.503019    -2.662364    -0.565284
    10           7         1.242681     1.099333    -0.090096
    11           6         2.172281     2.231172    -0.023257
    12           1         2.579968     2.335410     0.985293
    13           1         1.616822     3.127247    -0.293332
    14           1         2.991660     2.054559    -0.718927
    15           6        -0.135796     1.386111    -0.007792
    16           8        -0.579613     2.528266     0.068280
    17           6        -0.909480     0.175249    -0.059886
    18           7        -2.267047    -0.028070     0.012453
    19           6        -3.304449     0.997955     0.023792
    20           1        -4.268740     0.497905     0.127735
    21           1        -3.140128     1.677378     0.860273
    22           1        -3.276732     1.564934    -0.907811
    23           6        -2.444172    -1.380302     0.025878
    24           1        -3.430991    -1.822497     0.062448
---------------------------------------------------------------------
```

For the plot of the simulated Raman profile in figure 2, a Gaussian band shape function with a bandwidth (FWHM) of 5 cm^{-1} was used for the broadening. During this procedure, the Raman activities (S_i) calculated with the Gaussian 09 were converted to relative Raman Intensities (I_i) using the following relationship derived from the theory of Raman scattering[1]:

$$I_i = \frac{A(\nu_0 - \nu_i)^4 S_i}{\nu_i \left[1 - exp\left(-\frac{hc\nu_i}{kT} \right) \right]} \qquad [1]$$

where ν_0 is the excitation frequency (in cm^{-1} units), ν_i is he vibrational wavenumber of the ith normal mode, h is the Planck constant, c is the speed of light, k is the Boltzmann constant and A is a common normalization factor for all peak intensities.

4

Data analysis and fitting

The scattered light from the sample, polarized parallel ($I_\parallel$) and perpendicular ($I_\perp$) with respect to the incident radiation, was collected. Isotropic and anisotropic Raman intensity profiles were obtained according to the relation:

$$I_{iso} = I_\parallel - 4/3\, I_\perp \text{ and } I_{aniso} = I_\perp \tag{2}$$

The isotropic Raman spectral lines were fitted by a Kubo Anderson function (KAF).[2] Under this framework, the isotropic spectral shape for N vibrations can be represented by

$$I_{iso} = \sum_{i=1}^{N} A_i K_i\left(\omega, \omega_{0,i}, \sigma_i^2, \alpha_i\right) + B \tag{3}$$

where B is a constant background, A_i are scaling factors, and $K_i\left(\omega, \omega_{0,i}, \sigma_i^2, \alpha_i\right)$ is the KAF which can be expressed by the following equation

$$K_i\left(\omega, \omega_{0,i}, \sigma_i^2, \alpha_i\right) = \frac{e^{\alpha_i^2}}{\sigma_i} \sum_{n=0}^{\infty} \frac{(-\alpha_i^2)^n}{n!} \frac{\alpha_i + n/\alpha_i}{(\alpha_i + n/\alpha_i)^2 + \dfrac{(\omega - \omega_{0,i})^2}{\sigma_i^2}} \tag{4}$$

where σ_i^2 is the frequency second moment and its square root describes the frequency distribution of the active oscillator around the unperturbed frequency $\omega_{0,i}$ and $\alpha_i = \sigma_i \tau_{c,i}$ is a parameter which describes the modulation regime of the dephasing correlation time[3] and $\tau_{c,i}$ is the environmental modulation time of the perturbative events. This model predicts that if $\alpha \ll 1$, the modulation of the probe molecule is fast compared to the molecular perturbations of the system in which is embedded, and the original phase of the modulation is kept unaltered for a long time. In this particular case the KAF equation reduces to a Lorentzian function. Under these circumstances the vibrational dephasing relaxation time, τ_{vibr}, and the reorientational relaxation time τ_{reor}, can be calculated as:

$$\tau_{vibr} \cong \frac{1}{\sigma^2 \tau_c} = \frac{1}{\pi c \Gamma_{iso}}$$

[5a]

$$\tau_{reor} \cong \frac{1}{\pi c(\Gamma_{aniso} - \Gamma_{iso})}$$

[5b]

where c is the speed of light and Γ_i (i=iso, aniso) is the full width at half maximum of the Lorentzian for isotropic and anisotropic intensity modes, respectively.

The non coincidence effect, NCE, is defined as the non-coincidence of the position of the maxima of the isotropic and anisotropic Raman components:

$$\Delta v_{NCE} = v_{aniso} - v_{iso}$$

[6]

where v_{aniso} and v_{iso} are the normal mode peak frequency position obtained by fitting respectively the anisotropic and isotropic Raman profile with the above described procedure.

Figure S1 Isotropic spectra of caffeine aqueus solutions collected off-resonance (blue-lines) and on-resonance (pink lines, data at about 1550 cm^{-1} are affected by an experimental laser satellite artifact and therefore are omitted). On the top they are displayed the spectra recoreded on 1m caffeine aqueous solutions at 353 K. The high sensitivity of the resonance Raman scattering is shown in the panels at the bottom where extremely diuited solutions were measured at room temperature (0.01 m acquired at 532 nm, 0.0022 m acquired at 266 nm).
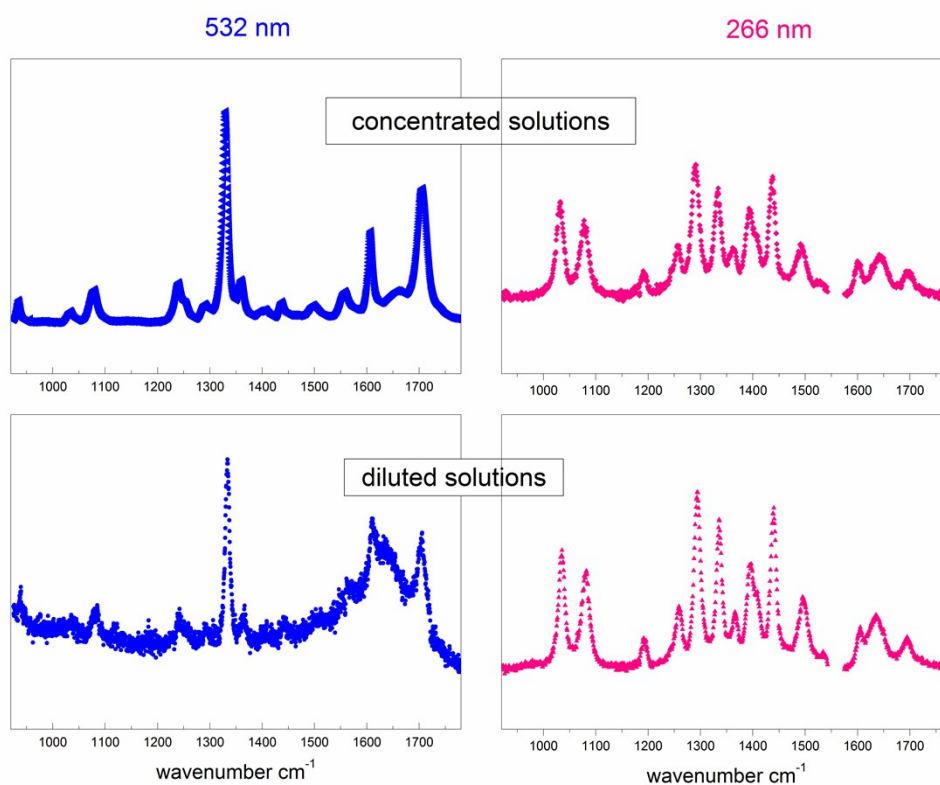
Figure S2 Concentration dependence of the isotropic peak position for the normal modes associated to: (top left) rocking C1M, stretching N3-C3M, stretching C6-N1-C2, bending C8-H8; (top right) rocking of the methyl groups, bending of the N-CH atoms and stretching of the C8-N7; (middle left) stretching of both the caffeine ring atoms; (middle right) stretching of the imidazole ring atoms; (bottom) in phase carbonyl stretching. Results obtained at 300K are displayed in light-blue, whereas results at 353K are reported in red.
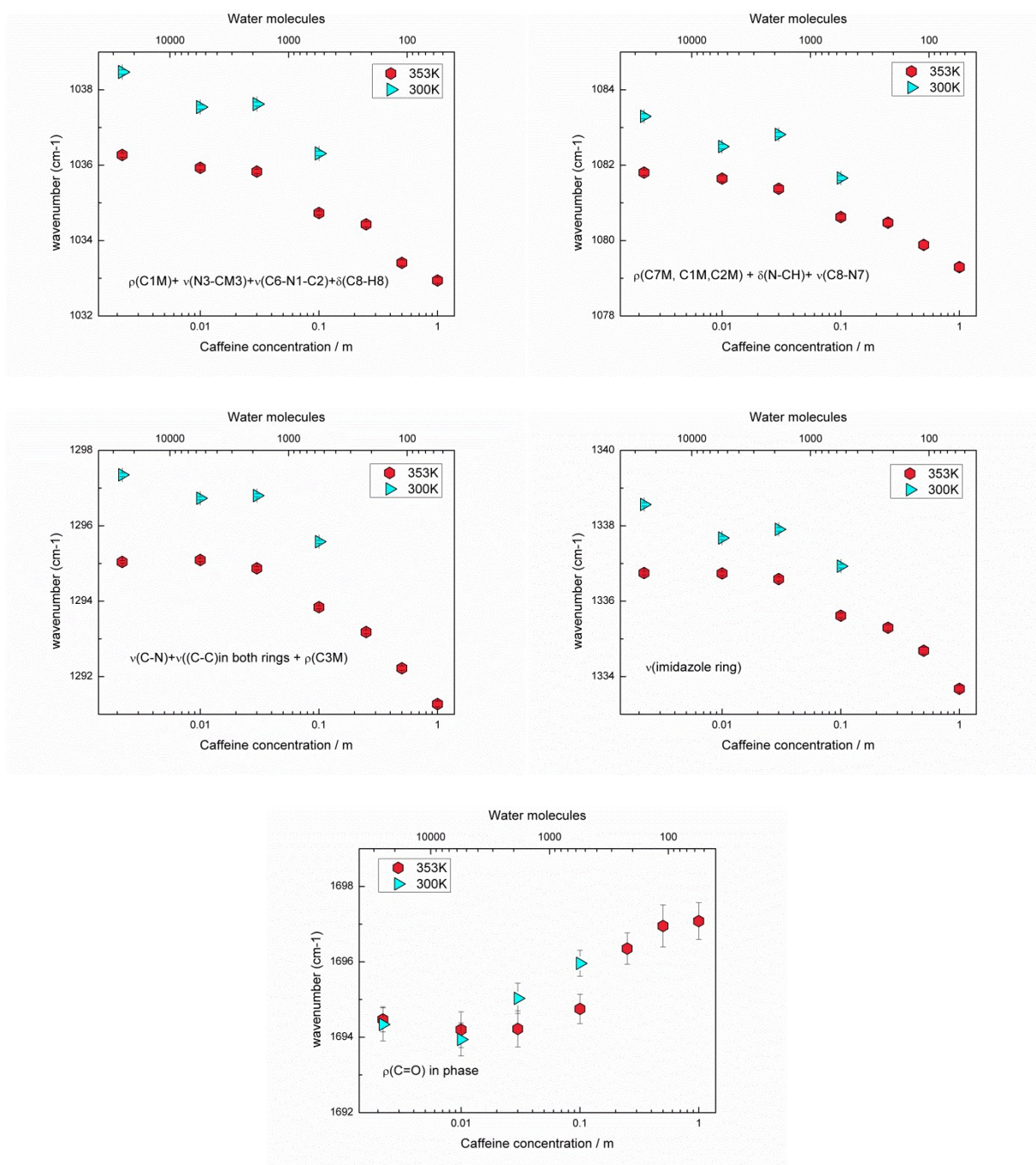
Figure S3 Experimental anisotropic and isotropic spectra in the frequency region of the totally symmetric breathing mode of the purine ring, ν_{rings}, and in that of the bending mode of methyl groups of caffeine, $\delta(CM)$. Anisotropic Raman spectra are displayed in red, whereas isotropic are in blue: a) 1 m caffeine aqueous solution at 353 K; b) 0.5 m caffeine aqueous solution at 353 K; c) 0.25 m caffeine aqueous solution at 353 K (dots: experimental data points; lines: fitting curves).
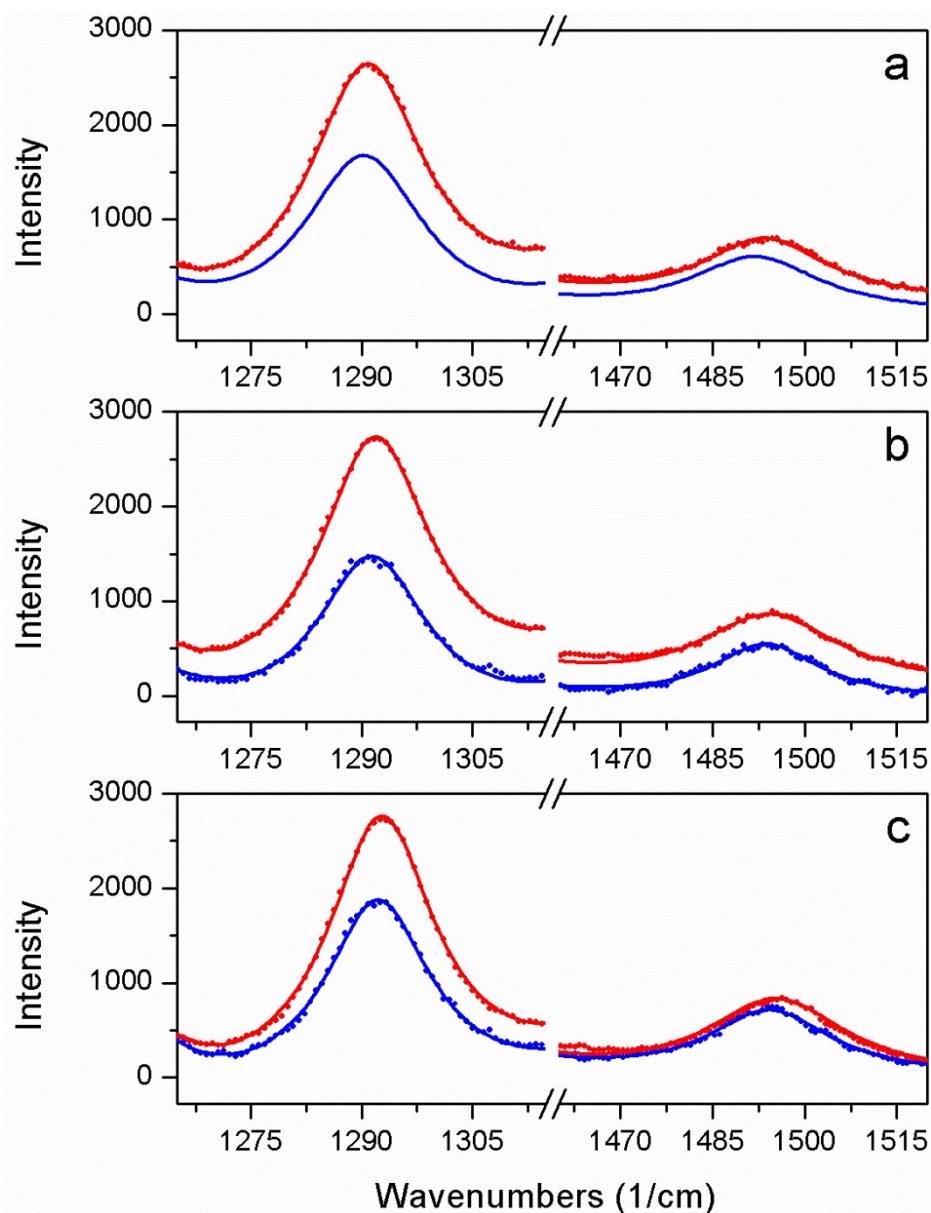
Figure S4 Optimized caffeine dimers structures. a) Parallel dimer, with a total dipole moment vector of ~6.76 D; b) Antiparallel dimer with a null total dipole moment vector. These optimized geometries were used as input for calculation of the Raman normal modes.
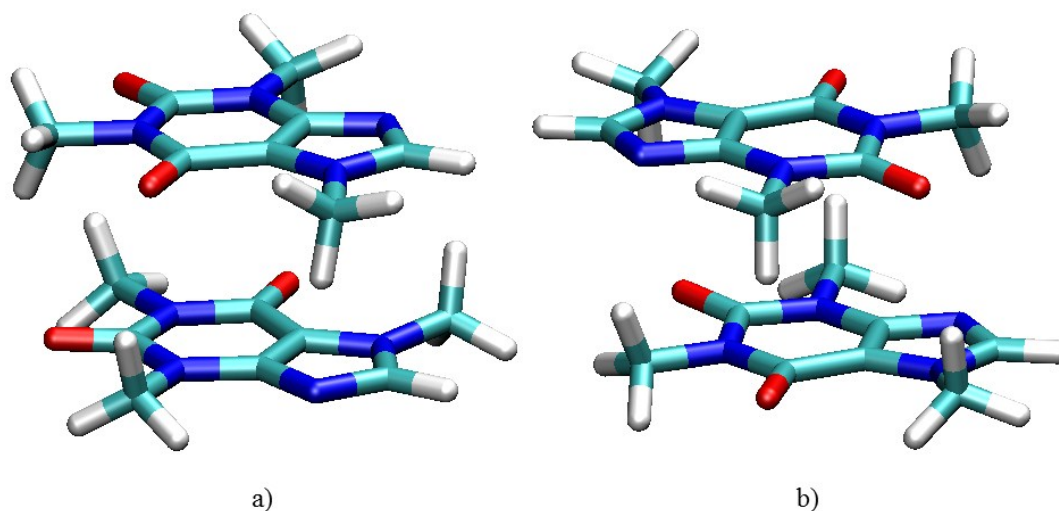

a)   b)

Table S3 Simulation results for the two caffeine dimers configurations, i.e. antiparallel and parallel. Wavenumbers (cm^{-1}), total Raman activity (S_{tot}), depolarization ratio (ρ), IR intensity, isotropic Raman activity (S_{iso}), anisotropic Raman activity (S_{aniso}) and frequency splitting of the coupled modes are reported. Isotropic and anisotropic Raman activities were calculated from the total Raman activity and the depolarization ratio using the expressions reported in Ref. 4. Vibrational normal modes for which it has been measured experimentally a significant NCE are highlighted.

ANTIPARALLEL DIMER							
	Wavenumbers cm^{-1}	S_{tot}	ρ	**IR**	S_{iso}	S_{aniso}	**Splitting** cm^{-1}
1	1030.16	5.1713	0.4674	9.00E-04	1.33E+00	3.84E+00	4.4
	1034.56	1.00E-04	0.6527	89.3539	7.85E-06	9.22E-05	
2	1079.92	3.4909	0.347	7.00E-04	1.39E+00	2.10E+00	0.68
	1080.60	0.0096	0.3385	0.1717	3.94E-03	5.66E-03	
3	1209.11	4.373	0.7271	0.1191	7.73E-02	4.30E+00	0.47
	1209.58	0.024	0.7173	21.6094	6.09E-04	2.34E-02	
4	1255.27	10.5653	0.2264	0.126	6.01E+00	4.55E+00	1.3
	1256.57	0.0092	0.2465	148.2726	4.95E-03	4.25E-03	
5	1271.16	0.2436	0.6884	3.222	1.19E-02	2.32E-01	0.36
	1271.52	15.3091	0.6953	0.0429	6.59E-01	1.47E+01	
6	1291.34	18.7578	0.5586	0.0098	3.07E+00	1.57E+01	1.89
	1293.23	0.0034	0.5606	42.0974	5.50E-04	2.85E-03	

	Wavenumbers cm⁻¹	S_tot	ρ	IR	S_iso	S_aniso	Splitting cm⁻¹
7	1343.32	40.9999	0.1701	0.0139	2.71E+01	1.39E+01	0.91
	1344.23	0.0112	0.1785	48.5086	7.24E-03	3.96E-03	
8	1381.34	66.6215	0.3174	2.00E-04	2.92E+01	3.75E+01	0.6
	1381.94	1.00E-04	0.3173	104.0669	4.38E-05	5.62E-05	
10	1403.34	7.3265	0.3767	0.2781	2.65E+00	4.68E+00	0.17
	1403.51	0.0781	0.3748	26.6514	2.84E-02	4.97E-02	
11	1442.26	0.0481	0.6354	18.4542	4.49E-03	4.36E-02	0.74
	1443.00	12.5603	0.6553	0.0667	9.58E-01	1.16E+01	
	1448.26	19.1952	0.7268	0.0047	3.44E-01	1.89E+01	2.07
	1450.33	6.00E-04	0.5754	64.1562	8.87E-05	5.11E-04	
	1460.56	0.3834	0.6365	43.9284	3.55E-02	3.48E-01	0.22
	1460.78	4.6026	0.6370	3.6822	4.24E-01	4.18E+00	
	1483.43	19.0966	0.7423	6.00E-04	1.13E-01	1.90E+01	1.79
	1485.22	4.00E-04	0.7145	73.2413	1.10E-05	3.89E-04	
	1493.40	9.2985	0.7386	0.0016	8.13E-02	9.22E+00	2.08
	1495.48	0.001	0.6964	196.0858	4.21E-05	9.58E-04	
12	1499.50	23.6664	0.6329	0.0041	2.26E+00	2.14E+01	1.25
	1500.75	0.0013	0.6717	7.3412	8.12E-05	1.22E-03	
	1504.34	12.4963	0.7202	0.0034	2.89E-01	1.22E+01	1.03
	1505.37	7.00E-04	0.5965	55.4525	8.97E-05	6.10E-04	
	1526.19	0.0108	0.7472	19.0465	2.31E-05	1.08E-02	1.18
	1527.37	11.377	0.7124	0.0083	3.33E-01	1.10E+01	
	1528.89	17.6976	0.6973	0.2003	7.33E-01	1.70E+01	0.09
	1528.98	0.7697	0.6915	4.2033	3.55E-02	7.34E-01	
	1535.81	11.3904	0.545	5.00E-04	2.02E+00	9.38E+00	0.94
	1536.75	4.00E-04	0.4249	22.1886	1.22E-04	2.78E-04	
13	1568.03	6.318	0.4233	0.0017	1.93E+00	4.38E+00	2.42
	1570.45	1.00E-04	0.3653	191.0331	3.76E-05	6.24E-05	
14	1609.58	51.5534	0.2236	0.0014	2.96E+01	2.20E+01	1.5
	1611.08	7.00E-04	0.2182	99.3652	4.07E-04	2.93E-04	
15	1690.21	20.4047	0.2424	0	1.11E+01	9.29E+00	11.96
	1702.17	0	0.3731	1258.9381	0.00E+00	/	
16	1734.85	68.3424	0.0957	0	5.44E+01	1.39E+01	6.61
	1741.46	0	0.4038	659.9526	0.00E+00	/	

PARALLEL DIMER

	Wavenumbers cm⁻¹	S_tot	ρ	IR	S_iso	S_aniso	Splitting cm⁻¹
1	1034.57	0.4868	0.7499	47.7733	3.71E-05	0.48676	0.88
	1035.45	4.626	0.3158	55.835	2.03537	2.59063	
2	1076.94	0.8067	0.7436	0.6518	0.00395	0.80275	0.07
	1077.01	2.5061	0.2616	0.0019	1.29357	1.21253	
3	1208.09	2.0256	0.75	17.2671	0	2.0256	0.97
	1209.06	0.6247	0.3766	5.9735	0.22593	0.39877	
4	1256.39	0.0155	0.7489	42.66	1.30E-05	0.01549	0.4
	1256.79	15.4552	0.4708	71.3785	3.91179	11.54341	
5	1267.33	0.7442	0.75	37.2218	0	0.7442	1.33
	1268.66	16.6562	0.3364	0.4313	6.8732	9.783	

6	1288.89	18.1037	0.5742	15.2625	2.69566	15.40804	1.37
	1290.26	0.578	0.75	17.3144	0	0.578	
7	1341.94	3.0414	0.75	13.3251	0	3.0414	2.32
	1344.26	38.0231	0.1388	33.5536	27.2096	10.8135	
8	1378.21	11.4889	0.75	0.5565	0	11.4889	0.59
	1378.80	41.9762	0.2367	102.2146	23.22998	18.74622	
10	1402.40	1.8796	0.7499	28.6897	1.43E-04	1.87946	0.22
	1402.62	5.4693	0.1015	0.1192	4.29335	1.17595	
11	1444.99	3.7594	0.5418	4.0665	0.67688	3.08252	2.32
	1447.31	10.9511	0.75	35.2543	0	10.9511	
	1451.16	9.7854	0.7042	32.8778	0.35064	9.43476	1.87
	1453.03	6.2253	0.75	25.9289	0	6.2253	
	1463.27	3.9092	0.6579	18.8976	0.28955	3.61965	0.56
	1463.83	0.4247	0.75	30.2057	0	0.4247	
	1483.81	9.3358	0.75	36.5184	0	9.3358	0.13
	1483.94	12.342	0.7389	41.1461	0.10504	12.23696	
	1495.12	0.0794	0.75	21.2622	0	0.0794	1.87
	1496.99	9.8393	0.745	114.1199	0.03759	9.80171	
12	1502.71	0.8069	0.75	5.4309	0	0.8069	0.05
	1502.76	24.7913	0.6605	10.1488	1.78165	23.00965	
	1506.01	4.2024	0.7122	55.2327	0.1237	4.0787	0.3
	1506.31	6.3247	0.75	17.4477	0	6.3247	
	1524.20	1.1801	0.75	7.0392	0	1.1801	2.61
	1526.81	0.7356	0.592	10.4238	0.09734	0.63826	
	1529.20	15.8082	0.6992	0.015	0.63014	15.17806	0.37
	1529.57	14.3007	0.75	15.8769	0	14.3007	
	1532.87	1.1577	0.75	19.1794	0	1.1577	1.89
	1534.76	2.5194	0.2894	0.1213	1.19997	1.31943	
13	1567.75	4.2925	0.75	5.1671	0	4.2925	2.62
	1570.37	0.9873	0.0331	209.5587	0.91349	0.07381	
14	1612.83	48.977	0.1939	25.4804	30.41696	18.56004	0.84
	1613.67	1.7514	0.7498	98.1697	2.67E-04	1.75113	
15	1696.59	38.8071	0.1315	116.9169	28.28363	10.52347	9.58
	1706.17	4.0306	0.75	1089.862	0	4.0306	
16	1742.52	2.0942	0.75	65.673	0	2.0942	3.96
	1746.48	48.5317	0.0803	603.7575	40.11439	8.41731	

Figure S5 Arrhenius temperature dependence of the reorientational relaxation time, the estimated activation energy E_a gives a value of 2.0 kcal mol^{-1} (± 0.4 kcal mol^{-1}).
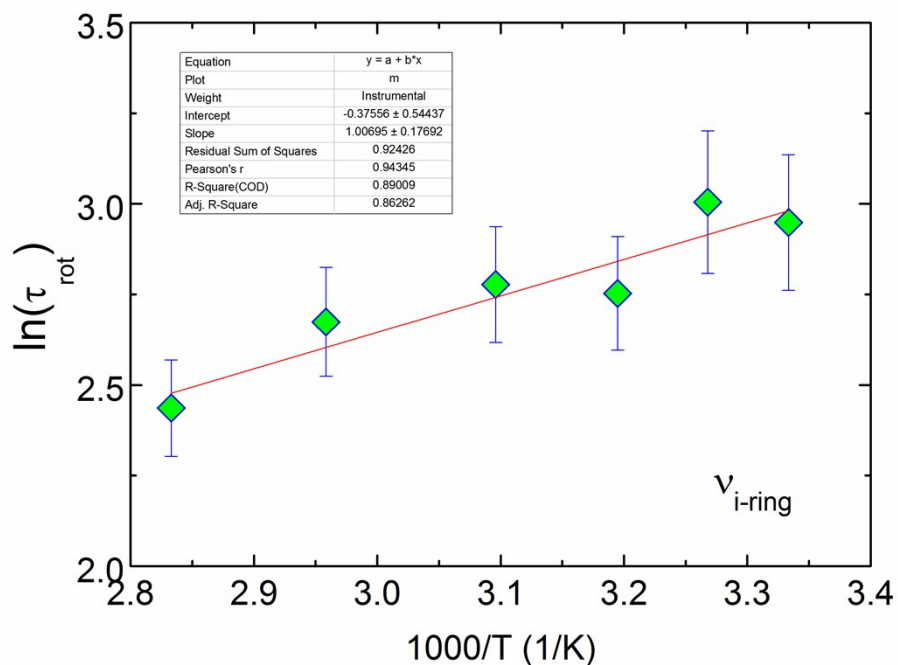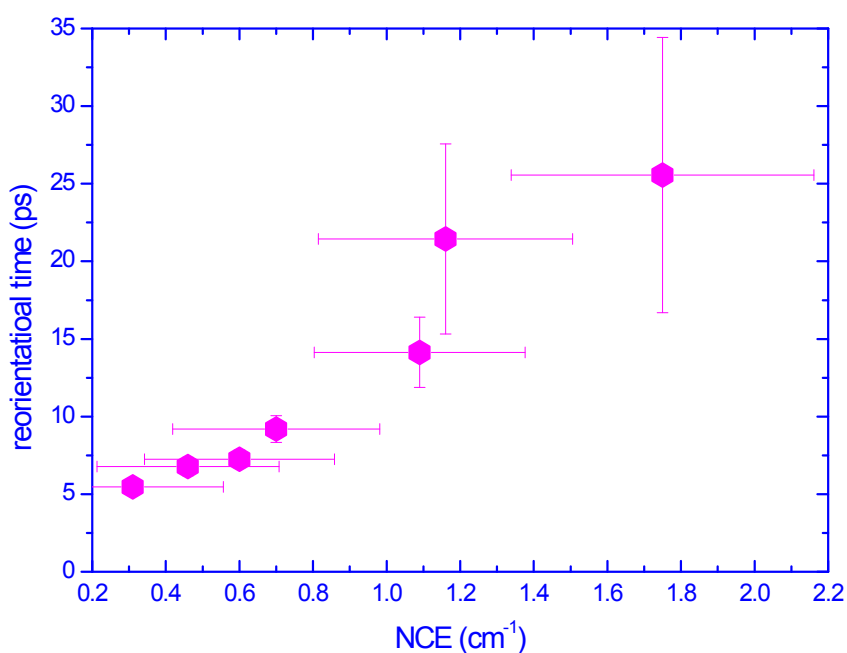

Figure S6 Correlation between the reorientational time and the non-coincidence effect associated to the vibrational normal mode involving the caffeine methyl groups bending.

References

1. V. Krishnakumar, G. Keresztury, T. Sundius and R. Ramasamy, *Journal of Molecular Structure*, 2004, **702**, 9-21.
2. L. Mariani, A. Morresi, R. S. Cataliotti and M. G. Giorgini, *The Journal of Chemical Physics*, 1996, **104**, 914-922.
3. W. G. Rothschild, *The Journal of Chemical Physics*, 1976, **65**, 455-462.
4. I. A. Heisler, K. Mazur, S. Yamaguchi, K. Tominaga, S. R. Meech, *Physical Chemistry Chemial Physics* 2011, **13**, 15573-15579.